Analysis of Torque Capability and Limits of Operation of AC Traction Motors on Sustainable High-Speed Electric Trains

CORNELIA A. BULUCEA[1] DORU A. NICOLA[1] MARC A. ROSEN[2]
NIKOS E. MASTORAKIS[3] CARMEN A. BULUCEA[4]
[1]Faculty of Electrical Engineering, University of Craiova
ROMANIA
[2]Faculty of Engineering and Applied Science, University of Ontario Institute of Technology
CANADA
[3]Military Institutes of University Education, Hellenic Naval Academy
GREECE
[4]Faculty of Medicine, University of Medicine and Pharmacy of Craiova
ROMANIA

Emails: abulucea@em.ucv.ro, dnicola@em.ucv.ro, marc.rosen@uoit.ca,
mastor@hna.gr, carmen.bulucea@umfcv.ro

Abstract: The sustainability of electric railway vehicles is related both to high energy efficiency and to mitigated environmental impact during all life stages (namely, production, use and end-of-life). It is widely accepted that the environmental performance of traction motor operation is closely related to its energy conversion efficiency. In line with this idea, sustainable operation of electric traction motors on railway systems represents a significant goal nowadays in the development of high power and high speed locomotives and trains. At present, high speed electric trains mostly work with three-phase induction motors or three-phase synchronous motors as traction motors. The two electric machine types have different efficiencies at different operation points, and experience differences with respect to safety, speed and power, energy use and exergy efficiency. An important issue that correlates these sustainability aspects is the electromagnetic torque developed by an electric traction motor, taking into consideration that the wide operating torque-speed range required to the electric railway vehicle imposes significant constraints on achieving a high efficiency of the traction motor. In order to provide an overview of the technical and environmental performance of the sustainable operation of electric trains, a detailed analysis is carried out of the electromagnetic torque capability of AC electric motors utilized as traction motors in modern locomotives of high power and/or high speed. The results of this work may help in enhancing the main criteria for optimising the high-efficiency operation of sustainable electric railway traction systems.

Key-Words: Electric railway system, electromagnetic torque, exergy, electric high-speed train, induction motor, sustainability, synchronous motor

1 Introduction

The final decades of the 20th century and the first decade of the 21st century were marked by a significant rise in the speed of electric railway vehicles due to progress in power electronics for electric locomotive technology [1-10]. Consequently, nowadays we are encountering a rethinking and redrawing of the architecture of electric railway vehicles, regardless of the type of the electric contact line (in DC or in AC).

Nonetheless, concerns and questions have been raised regarding the sustainability of electric railway transportation systems, especially considering the environmental impact of the transport sector [1-11]. In line with this idea, international legislation has required the technical and environmental aspects to be merged, according to Life Cycle Assessment, which includes all life stages of a technical system, namely the production, the use and the end of life phases. In the case of electric vehicles the literature

[1-11] shows that the environmental performance of the electric traction motor operation is closely linked to its energy conversion efficiency. Following this notion, under the vision of sustainable development and industrial ecology, the key points of operation of electric railway vehicles nowadays are related to the high electromagnetic torque developed by traction motors, energy savings and environmental impact mitigation, particularly through high exergy efficiency [6-7, 11-13]. Moreover, the variable voltage/current variable frequency (VV/CVF) power conversion technology facilitates the use of on-board AC drives which ensure regenerative braking and thus make possible efficient management of energy supply of high speed trains [6-11,14]. But note that these advantages are met under the condition of using in traction drives the AC electric motors, namely of induction type or synchronous type, regardless of the contact line type.

The rivalry between the two three-phase AC traction electric motors, namely the induction motor and synchronous motor persists, each competing to be the safest, fastest and cheapest [1-14]. The two electric machine types have different efficiencies at different operation points in terms of electromagnetic torque [1-14]. An accurate insight into these two types of electric traction motors (three-phase induction motors and three-phase synchronous motors) is presented subsequently.

The three-phase induction motor with squirrel-cage rotor meets the criteria for an ideal traction motor, since it is robust and reliable, having fewer components than the DC traction motor. Moreover, for this type of electric motor the energy transfer between the stator and the rotor is performed without an electric contact, but instead just through the electromagnetic field, so that there are no limitations with respect to power, speed or voltage. Note that switching to the braking regime, or sense reversal, are achieved through the control logic of the power converters, without electromechanical contactors [5-6,9-11].

Further, a comparison of the traction motor with collector shows that the three-phase induction motor with a cage rotor presents an advantage in that, for the same useful power, the size and weight are lower.

The traction induction motors used on the locomotives and high speed/power trains are robust, with rated powers up to 1.5 MW. As a traction motor the induction motor must satisfy several criteria [5-6,8-11]:

- high torque developed at low speeds, even during start-up,
- high energy efficiency and cost effectiveness, and
- operation over a large range of the supply frequency, from roughly 0.4–1 Hz to 140–180 Hz, both as a motor and as a brake (generator).

The technology becomes significantly complicated in the range of low frequencies (under the rated frequency) because the motor is submitted to magnetic saturation at relatively small variations of supply voltage. For this reason, in the under-rated frequency range, the voltage will vary simultaneously with the supply frequency, in order to enable through the control system both the appropriate level of magnetic stresses and the required magnitude of the electromagnetic torque [5, 8-11].

But developments should be made in the range of over-rated frequencies for which, due to reasons of motor windings insulation and voltage stresses of power electronics, the supply voltage must be maintained constant at the level of rated voltage U_N. Consequently, when powered at the rated voltage U_N and over-rated frequencies, the induction motor operates with weakened flux, which leads to the torque overloading capability λ_M becoming increasingly lower and the rotor pulsation ω_r becoming increasingly higher. Besides, for the operation in the range of over-rated frequencies, the reaching of critical rotor pulsation ω_{rk} limits the higher value of the stator frequency to below the maximum f_{smax} [5-6, 8-11].

The synchronous motor utilized as traction motor must develop significant high electromagnetic torques at variable speeds, namely from the starting to the maximum speed. Consequently it is compulsory the traction synchronous motor to be powered from a static converter with variable frequency so that the rotor, which controls the static converter to maintain the synchronization with the rotating magnetic field at any value of stator frequency [1, 8-9].

Following this idea means that the current converters with natural commutation which power the self-controlled three-phase traction synchronous motors are simple, being composed by six thyristorised branches connected as a three-phase bridge. Note that some problems concerning the natural commutation realisation appear at very low speeds, when the magnitude of the counter electromotive force (c.e.m.f) is small (insufficient to ensure the commutation). In such situations, from the starting regime up to roughly 5-10% of the maximum speed v_{max}, assisted commutation is necessary [5, 15-16].

The self-controlled synchronous motor becomes competitive as a traction motor solely at high powers, which is exactly in the application field of electric railway locomotives/trains. Specifically, three-phase traction synchronous motors with unit powers up to 1300 kW (in continuous operation regime) with forced ventilation are manufactured, of axial type (being provided with axial channels in the stator ferromagnetic core).

In this study, we perform a detailed analysis of the electromagnetic torque developed by the three-phase induction motor and the three-phase synchronous motor, the most generally used traction AC electric motors in present-day railway systems. We focus here on these two types of AC motors, which are widely used as traction motors on electric railway transportation systems, with particular reference to electromagnetic torque analysis, since certain traits of the developed electromagnetic torque are strongly related to the safety, speed, exergy efficiency and energy savings of high power and speed locomotives and trains. The aim of this study is to enhance understanding of these motors and their use in railway systems. Consequently, we present in the paper some less known theoretical aspects of the operation at variable frequency of AC traction motors.

2 Analysis of Electromagnetic Torque Developed by Traction Induction Motor

To address meaningfully many of the problems facing railway vehicles, conditions for the performance of sustainable transportation systems must be formulated [1-11]. Costs should reflect value, which is doubtless associated with sustainability aspects [12-14]. The sustainability of traction operation of the electric induction motor is related its exergy efficiency.

In physics and engineering, work is a specific form of action, and exergy is defined based on work, i.e. ordered motion, or ability to perform work [6-7,11-13]. While energy is a measure of quantity only, exergy is a measure of quantity and quality or usefulness. Since exergy is a measure of the potential of a system to do work, the electromagnetic torque M developed by an induction motor can be interpreted as the driving force of useful work, i.e. the electric motor output exergy [1,5-7,11].

In line with this idea, through the modeling of the electromagnetic torque developed by induction motor, this study supports the findings that electric traction drive systems using induction motors fed by VVVF inverters enhance the sustainable operation of railway trains.

In order to assess the electromagnetic torque developed by the traction induction motor, the vehicle regulation speed is determined by examining the VVVF inverter and electric machine as an assembly [1,5]. We have pointed out in previous studies [1,6-7,11,14] that a traction electric vehicle might be analyzed as an ecosystem, and the dynamic regimes in electric train operation, e.g. starting or braking processes, can be viewed as representing the industrial ecosystem movement among points of equilibrium. Since the traction motor speed regulation is based on stator voltage and frequency variation, in order to achieve high energy and exergy efficiencies, the first requirement of the train control system concerns passing of the motor operation equilibrium point from one mechanical characteristic to another [1,11,13].

If we note by $s = \frac{n_s - n}{n_s} = \frac{\omega_r}{\omega_s} = \frac{f_r}{f_s}$ the slip of rotor (having the speed n) in the rotating magnetic field (which has the synchronism speed $n_s = 60 \cdot f_s/p$), then the electromagnetic torque M developed by the traction induction motor at any current value of the stator frequency f_s and rotor slip s (respectively, rotor pulsation $\omega_r = s \cdot \omega_s$) is specified by $M = \frac{3p}{\omega_s} \cdot \frac{R_r'}{s} \cdot I_r'^{\,2} = 3p \cdot \frac{R_r'}{\omega_r} \cdot I_r'^{\,2}$.

Neglecting the stator resistance ($R_s \approx 0$), the evaluation relation of the electromagnetic torque M becomes:

$$M = M(\omega_s, \omega_r) = 3p \cdot \frac{1-\sigma}{\sigma \cdot L_s} \cdot \frac{\left(\frac{U_s}{\omega_s}\right)^2}{\frac{R'_r}{\omega_r \cdot \sigma \cdot L'_r} + \frac{\omega_r \cdot \sigma \cdot L'_r}{R'_r}} \quad (1)$$

With the notation $\omega_m = p \cdot \Omega_m = p\frac{2\pi \cdot n}{60}$, the torque characteristic of the induction motor, meaning the curve $M = f(\omega_m)$ for any constant pulsation/frequency $\omega_s = 2\pi f_s = ct.$ and $\omega_m = \omega_s - \omega_r$ is graphically illustrated in Figure 1.

The specific points of the mechanical characteristic in Figure 1 have coordinates (for any constant value of the stator frequency f_s) given by:

- mechanical pulsation ω_m corresponding to the synchronism point (when $\omega_r = 0$) :

$$\omega_m = \omega_s = 2\pi \cdot f_s = 2\pi \frac{p \cdot n_s}{60} \quad (2)$$

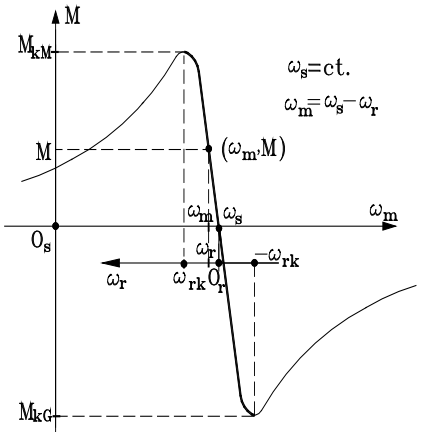

Figure 1. Mechanical characteristic M = f(ω_m) at ω_s=ct.

- critical rotor pulsations ω_{rk} (extreme points' abscissa of the graph in Figure 1):

$$\omega_{rk} = \omega_{rk\psi s} = \pm \frac{R'_r}{\sigma \cdot L'_r} \tag{3}$$

- extreme values (as motor M_{kM} and respectively as generator M_{kG}, of the torque curve), given by:

$$M_k = M_{k\psi_s} = \pm \frac{3p}{2} \cdot \frac{1-\sigma}{\sigma \cdot L_s} \cdot \left(\frac{U_s}{\omega_s}\right)^2 \tag{4}$$

Note in the above relation that the sign "+" refers to the motor regime (with index M in Figure 1) while the sign "-" refers to the generator regime (with index G in Figure 1).

2.1 Operation at Variable Frequency and Controlled Flux of the Induction Motor

The operation at variable frequency with controlled flux is preceded for induction motors in drive systems with vectorial control [5,8-9,11,17-18]. The vectorial regulation and control method is based on space phasor theory, taking into consideration the control of both the flux and the induction machine electromagnetic torque M. In principle, the stator current space phasor is decomposed into two perpendicular components (a flux component and a torque component) which are separately controlled. One could analyze the permanent harmonics regime of variable frequency operation with controlled stator flux, controlled useful flux or controlled rotor flux. As an example, we present the operation with controlled stator flux [5,18].

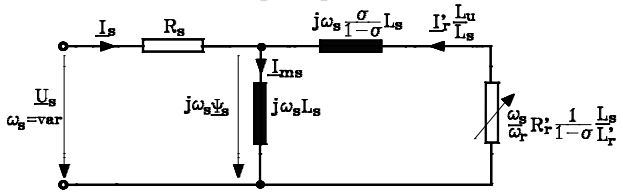

Figure 2. Electric circuit (modified) for induction motor

From equations of the electric circuit (see Fig. 2) the following relations can be derived for the stator current components [5-6,18]:

$$I_{sx} = \frac{\psi_s}{L_s} + \frac{1-\sigma}{\sigma L_s} \frac{\psi_s}{\frac{R'_r}{\omega_r \sigma L'_r} + \frac{\omega_r \sigma L'_r}{R'_r}} \frac{\omega_r \sigma L'_r}{R'_r} \tag{5}$$

$$I_{sy} = \frac{1-\sigma}{\sigma L_s} \frac{\psi_s}{\frac{R'_r}{\omega_r \sigma L'_r} + \frac{\omega_r \sigma L'_r}{R'_r}}$$

The absolute value of the stator current can be determined with the formula $I_s = (I_{sx}^2 + I_{sy}^2)^{1/2}$.

Within an ecological framework, the electromagnetic torque M is related to the system output exergy. We can express M in complex coordinates axes system (oriented on $\underline{\psi}_s$) as

$$\begin{aligned} M &= 3p \cdot Im\{\underline{I}_s \cdot \underline{\psi}_s^*\} = \\ &= 3p \cdot Im\{(I_{sx} + jI_{sy}) \cdot \psi_s\} = \\ &= 3p \cdot \psi_s \cdot I_{sy} \end{aligned} \tag{6}$$

Substituting I_{sy} from (14), the torque relation becomes

$$M = 3p \cdot \frac{1-\sigma}{\sigma L_s} \cdot \frac{\psi_s^2}{\frac{R'_r}{\omega_r \sigma L'_r} + \frac{\omega_r \sigma L'_r}{R'_r}} \tag{7}$$

If the stator flux ψ_s is constant, the electromagnetic torque magnitude depends on the rotor current pulsation ω_r but not the stator supply frequency f_s. The torque curve M=f(ω_r) at ψ_s=const. is not linearly dependent on ω_r, having two symmetrical extremes:

$$\begin{aligned} &\frac{\partial M}{\partial \omega_r} = 0;\ \omega_{rk\psi_s} = \pm \frac{R'_r}{\sigma \cdot L'_r}; \\ &M_{k\psi_s} = M(\omega_{rk\psi_s}) = \pm \frac{3p}{2} \cdot \frac{1-\sigma}{\sigma \cdot L_s} \cdot \psi_s^2 \end{aligned} \tag{8}$$

The dependence of M=f(ω_r) at ψ_s=const. is shown in Fig. 3.

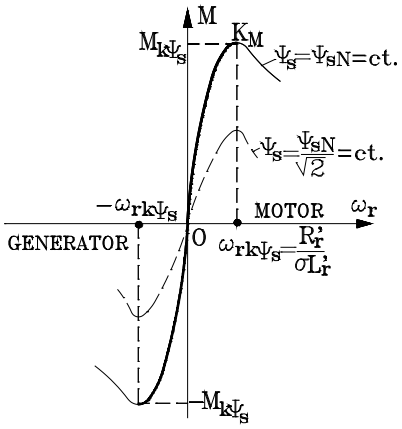

Figure 3.Torque characteristic M=f(ω_r) at controlled stator flux

In a steady-state regime, stable system operation (with $\partial M/\partial\omega_r>0$) is performed only on the ascendant zone of the characteristic $M=f(\omega_r)$ in Fig. 3 and corresponds at small rotor pulsations to the condition $|\omega_r| \le \omega_{rk\psi s}$. The mechanical characteristics family $M=f(n)$ of the induction motor operating at ψ_s=const., for different stator frequencies f_s, are shown in Fig. 4.

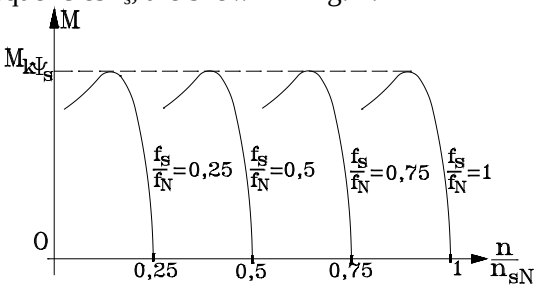

Figure 4. Mechanical characteristics $M=f(n)$ at ψ_s=const. for different frequency f_s values ($f_s \le f_N$)

The constant stator flux magnitude ψ_s for any stator frequency f_s and torque M (respectively, any rotor pulsation ω_r) imposes an exact control of either the supply voltage U_s or the supply current I_s. We see again an analogy between this electrical system and an ecosystem. An appropriate technical system control must be achieved for reducing exergy destruction when the equilibrium point passes from one stable state (represented by the operation point on a certain mechanical characteristic) to another stable state (on another mechanical characteristic). This observation implies the system control needs to be assessed next.

2.1.1 Torque Capability and Comparison at Constant Flux Operation

Note that, at any frequencies, in the permanent harmonic regime, among the fluxes $\underline{\Psi}_s$, $\underline{\Psi}_u$, $\underline{\Psi}'_r$ and the currents $\underline{I}_s$, $\underline{II}'_r$ of any unsaturated induction machine with electric and magnetic symmetry, the following relations apply [1,5, 7,11]:

$$\begin{aligned} \underline{\psi}_s &= L_{s\sigma}\cdot\underline{I}_s + \underline{\psi}_u \\ \underline{\psi}_s &= \sigma\cdot L_s\cdot\underline{I}_s + \frac{L_u}{L_{r'}}\cdot\underline{\psi}'_r \\ \underline{\psi}'_r &= \underline{\psi}_u + L'_{r\sigma}\cdot\underline{I}'_r \\ 0 &= R'_r + j\,\omega_r\cdot\underline{\psi}'_r \end{aligned} \qquad (9)$$

Accordingly, a phasor diagram is shown in Fig. 5 of the fluxes and currents for the induction machine operating in the motor regime. In the complex reference system, with real axis (+1) along the direction of phasor $\underline{\Psi}'_r$ (with $\underline{\Psi}'_r=\Psi'_r+j\cdot 0$; $\underline{I}_s=I_{sx}+j\cdot I_{sy}$ and $\underline{I}'_r=0-j\cdot I'_r$), from the geometry of the rectangular triangles OAA' and OBB' (see Fig. 5) one can write:

$$\psi_s^2 = [\frac{L_u}{L_{r'}}\cdot\psi'_r + \sigma\cdot L_s\cdot I_{sx}]^2 + (\sigma\cdot L_s\cdot I_{sy})^2 \qquad (10)$$

$$\psi_u^2 = \psi'^2_r + (L'_{r\sigma}\cdot I'_r)^2$$

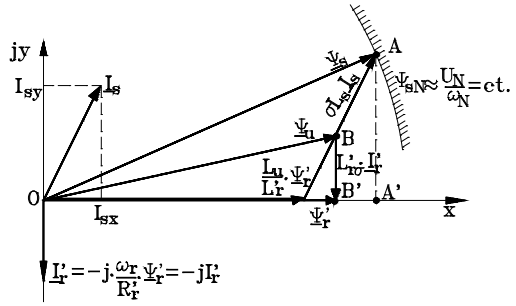

Figure 5. Phasor representation of induction motor fluxes and currents at $\omega_r>0$

Furthermore, taking into consideration the components I_{sx} and I_{sy}, as well as the rotor current I'_r in accordance with the following relations:

$$I_{sx}=\frac{\psi'_r}{L_u};\ I_{sy}=\frac{\psi'_r}{L_u}\cdot\frac{L'_r}{R'_r}\cdot\omega_r;\ I'_r=\frac{\omega_r}{R'_r}\cdot\psi'_r \qquad (11)$$

and after mathematical calculations, the expressions for the fluxes Ψ_u and Ψ'_r can be determined:

$$\begin{aligned} \psi_u(\omega_r) &= \psi_s\cdot\frac{L_u}{L_s}\cdot\sqrt{\frac{1+(\frac{L'_{r\sigma}}{R'_r}\cdot\omega_r)^2}{1+(\frac{\sigma\cdot L'_r}{R'_r}\cdot\omega_r)^2}} \\ \psi'_r(\omega_r) &= \psi_s\cdot\frac{L_u}{L_s}\cdot\frac{1}{\sqrt{1+(\frac{\sigma\cdot L'_r}{R'_r}\cdot\omega_r)^2}} \end{aligned} \qquad (12)$$

Note that the fluxes Ψ_u and Ψ'_r depend on Ψ_s, as well on machine parameters and on ω_r. But any induction machine designed to be supplied with phase voltage U_N at stator frequency f_N ($\omega_N = 2\pi\cdot f_N$) will have the stator flux Ψ_s approximately constant, with magnitude Ψ_{sN}, where:

$$\psi_{sN}\approx\frac{U_N}{\omega_N}=ct. \qquad (13)$$

Hence, for operation with constant stator flux ($\Psi_s = \Psi_{sN}$ = ct.), the reference levels of the fluxes Ψ_u=ct. and Ψ'_r = ct., respectively should set to values such that, over the entire variation range of rotor pulsation ω_r, the stator flux Ψ_s does not exceed the established limit value. Therefore, in Fig. 6 there are shown the dependence $\Psi_s=\Psi_{sN}$=ct. in accordance with (13) and $\Psi_u = f_1(\omega_r)$ and $\Psi'_r = f_2(\omega_r)$ according to (12) for the maximum variation range of ω_r ($|\omega_r| \le R'_r/L'_{r\sigma}$ when the induction machine has stable operation at Ψ_u=ct.).

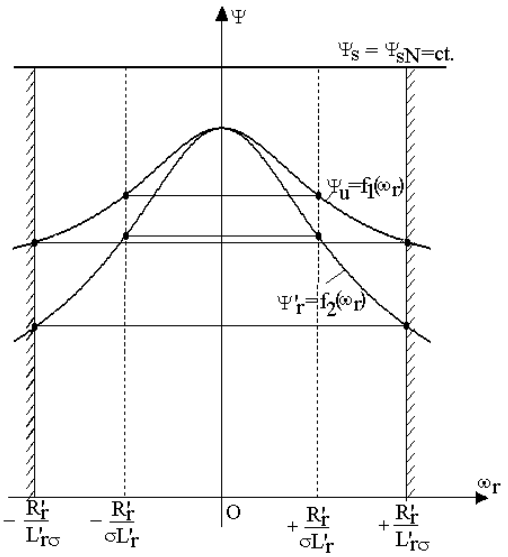

Figure 6. Dependence of induction machine fluxes Ψ_s, Ψ_u and Ψ'_r on ω_r

Based on the curves of Fig. 6 and the above relations, the constant flux levels are determined:

$$\psi_s = \psi_{sN} = ct. \tag{14}$$

$$\psi_u = f_1(\pm\frac{R'_r}{L'_{r\sigma}}) = \psi_s \cdot \frac{L_u}{L_s} \cdot \frac{\sqrt{2}}{\sqrt{1+(\frac{\sigma L'_r}{L'_{r\sigma}})^2}} = ct.$$

$$\psi'_r = f_2(\pm\frac{R'_r}{L'_{r\sigma}}) = \psi_s \cdot \frac{L_u}{L_s} \cdot \frac{1}{\sqrt{1+(\frac{\sigma L'_r}{L'_{r\sigma}})^2}} = ct. \quad (\psi'_r = \frac{\psi_u}{\sqrt{2}})$$

For these constant values of fluxes Ψ_s, Ψ_u and Ψ'_r, an exergetic analysis imposes the electromagnetic torque characteristics $M = f(\omega_r)$, and stator current characteristics $I_s = f(\omega_r)$ are compared for the stable operation intervals.

2.1.1.1 Electromagnetic torques comparison at Ψ_s = ct., Ψ_u=ct. and Ψ'_r = ct.

For the three subsequent cases, the electromagnetic torque M has the following expressions:

a) When stator flux is constant Ψ_s = ct.:

$$M = \frac{2 \cdot M_{k\psi_s}}{\frac{\sigma \cdot L'_r \cdot \omega_r}{R_{r'}} + \frac{R_{r'}}{\sigma \cdot L'_r \cdot \omega_r}} \tag{15}$$

$$M_{k\psi_s} = \frac{3p}{2} \cdot \frac{1-\sigma}{\sigma \cdot L_s} \cdot \psi_s^2$$

b) When useful flux is constant Ψ_u = ct.:

$$M = \frac{2 \cdot M_{k\psi_u}}{\frac{L'_{r\sigma} \cdot \omega_r}{R'_r} + \frac{R'_r}{L'_{r\sigma} \cdot \omega_r}} \tag{16}$$

$$M_{k\psi_u} = \frac{3p}{2} \cdot \frac{1}{L'_{r\sigma}} \cdot \psi_u^2$$

c) When rotor flux is constant Ψ'_r = ct.:

$$M = 3p \cdot \frac{\omega_r}{R'_r} \cdot \psi'^2_r \tag{17}$$

Moreover, according to the constant flux levels (14), between the maximum torques $M_{k\Psi s}$ and $M_{k\Psi u}$ the following recurrence relationship can be demonstrated:

$$\frac{M_{k\psi_s}}{M_{k\psi_u}} = \frac{1}{2} \cdot (\frac{\sigma \cdot L'_r}{L'_{r\sigma}} + \frac{L'_{r\sigma}}{\sigma \cdot L'_r}) \tag{18}$$

Also, since the electromagnetic torque is interpreted as output exergy, based on the observation $\Psi'_r = \Psi_u/\sqrt{2}$ = ct., at Ψ'_r = ct. a relationship for the electromagnetic torque M can be useful within the exergetic analysis:

$$M = M_{k\psi_u} \cdot \frac{L'_{r\sigma}}{R'_r} \cdot \omega_r \tag{19}$$

Graphically, curves of the induction machine electromagnetic torque $M/M_{k\Psi s} = f(\omega_r)$ at Ψ_s = ct., Ψ_u = ct., and Ψ'_r = ct., respectively, are presented in Fig. 7.

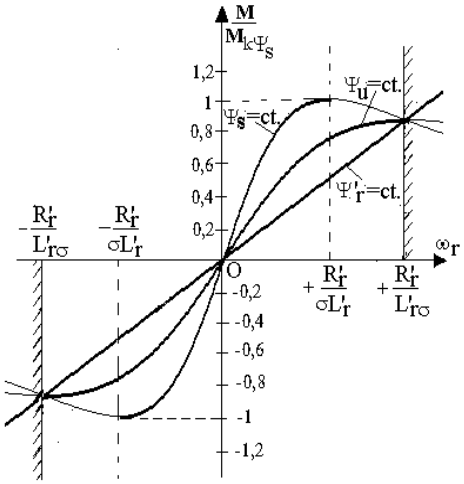

Figure 7. Curves of $M/M_{k\Psi s}=f(\omega_r)$ at constant flux

2.1.1.2 Stator currents comparison at Ψ_s = ct., Ψ_u=ct. and Ψ'_r = ct.

According to relationship (14) for constant flux levels, the stator current I_s expressions become as follows:

a) When stator flux is constant Ψ_s = ct.:

$$I_s = \frac{\psi_s}{L_s} \cdot \sqrt{\frac{1+(\frac{L'_r}{R'_r} \cdot \omega_r)^2}{1+(\frac{\sigma \cdot L'_r}{R'_r} \cdot \omega_r)^2}} \tag{20}$$

b) When useful flux is constant Ψ_u = ct.:

$$I_s = \frac{\psi_s}{L_s} \cdot \frac{\sqrt{2}}{\sqrt{1+(\frac{\sigma \cdot L'_r}{L'_{r\sigma}})^2}} \cdot \sqrt{\frac{1+(\frac{L'_r}{R'_r} \cdot \omega_r)^2}{1+(\frac{L'_{r\sigma}}{R'_r} \cdot \omega_r)^2}} \quad (21)$$

c) When rotor flux is constant Ψ'_r = ct.:

$$I_s = \frac{\psi_s}{L_s} \cdot \frac{1}{\sqrt{1+(\frac{\sigma \cdot L'_r}{L'_{r\sigma}})^2}} \cdot \sqrt{1+(\frac{L'_r}{R'_r} \cdot \omega_r)^2} \quad (22)$$

Graphically, in Fig. 8 there are depicted the characteristics of stator current I_s at Ψ_s = ct., Ψ_u = ct., and Ψ'_r = ct., respectively.

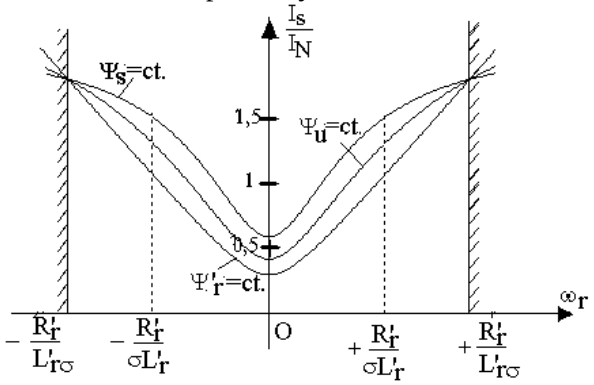

Figure 8. Characteristics of $I_s/I_N=f(\omega_r)$ at constant flux

2.1.1.3 Discussion of torques

The greatest magnitudes of electromagnetic torque are obtained when operating at Ψ_s=ct. Moreover, with the usual approximations $\sigma \cdot L'_r = L_{s\sigma} + L'_{r\sigma}$ and $L'_{r\sigma} \_ L_{s\sigma}$, the maximum torque relationship is obtained in the form:

$$M_{k\psi_u} \approx \frac{4}{5} \cdot M_{k\psi_s} \quad (23)$$

This emphasizes that the maximum electromagnetic torque in operating at Ψ_u = ct. is approximately with 20% smaller than the maximum torque in operating at Ψ_s = ct. The ratio of the critical rotor pulsations $\omega_{rk\psi s}$ and $\omega_{rk\psi u}$ is:

$$\frac{\omega_{rk\psi_s}}{\omega_{rk\psi_u}} = \frac{L'_{r\sigma}}{\sigma \cdot L'_r} \approx \frac{1}{2} \quad (24)$$

This means that an "inferior" maximum torque $M_{k\Psi u}$ is developed at the rotor pulsation with a double value that of the rotor pulsation corresponding to $M_{k\Psi s}$ ($\omega_{rk\Psi u} = 2 \cdot \omega_{rk\Psi s}$).

Moreover, at the imposed electromagnetic torque, the smallest value of rotor pulsation is obtained in operation with Ψ_s = ct.

From Fig. 8, similar observations are drawn with regard to the stator currents. Actually, the smallest values of stator currents I_s are obtained for operation with Ψ'_r = ct.

The analysis of induction machine operation with constant flux highlights that only at Ψ'_r = ct. do the mechanical characteristics not have extremum points; they are straight lines. These linear characteristics are preferable for applications which demand high sustainability dynamics in induction machine operation.

2.2 Limits of Variation of Stator Frequency

For the supply with variable frequency voltages it is important to assess the limit values of stator minimum frequency f_{smin} and maximum frequency f_{smax} (as in Figure 9, in the bottom part) among which the stable operation of the traction induction machine is possible.

2.2.1 Minimum Stator Frequency

The minimum frequency (for operation with constant stator flux, see Figure 9) is assessed taking into consideration that in a steady-state regime, at any value of stator frequency f_s, among rotor pulsation ω_r, stator pulsation $\omega_s = 2\pi \cdot f_s$ and mechanical pulsation $\omega_m = p \cdot \Omega_m = p \cdot 2\pi \cdot n/60$, the "Frequency Theorem" relation is valid:

$$\omega_s = \omega_m + \omega_r \quad (25)$$

or

$$2\pi \cdot f_s = p \cdot \frac{2\pi \cdot n}{60} + \omega_r \quad \Rightarrow \quad n = \frac{60}{p} \cdot (f_s - \frac{1}{2\pi} \cdot \omega_r) \quad (26)$$

For any stator frequency $f_s < f_N$, the rotor speed n_k corresponding to maximum electromagnetic M (meaning the abscissa of point K_M in Figure 9) is established with the relation:

$$n_k = \frac{60}{p} \cdot (f_s - \frac{1}{2\pi} \cdot \omega_{rk\psi_s}); \qquad n_k \geq 0 \quad (27)$$

The minimum stator frequency f_{smin} (that still will ensure the above operation conditions) corresponds to the limit situation when n_k = 0. That means that the minimum stator frequency will be given by the relation:

$$f_{smin} = \frac{1}{2\pi} \cdot \omega_{rk\psi_s} = \frac{1}{2\pi} \cdot \frac{R'_r}{\sigma \cdot L'_r} \quad (28)$$

Note that f_{smin} must be ensured by the supply source (VVVF) and depends solely on the parameters R'_r, L'_r and σ of the traction induction machine.

In Figure 9, the smooth starting manner (without shocks) is highlighted, through a progressive increase of the stator flux ψ_s (from 0 up to ψ_{sN}) at the minimum value f_{smin} = ct. (of the supply stator frequency), followed by an increase of the stator frequency f_s (at the constant stator flux a $\psi_s = \psi_{sN}$ = ct.) simultaneously with the increase of rotor speed.

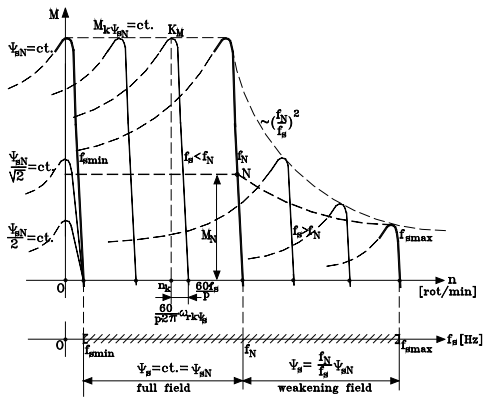

Figure 9.Overview of traction induction motor characteristics for operation at variable stator frequency f_s

2.2.2 Maximum Stator Frequency

The maximum stator frequency $f_{s\max}$ (higher than f_N) will be established by the condition of development (still) of an electromagnetic power P_M of magnitude equal to that of the motor rated operation.

Note that because of the voltage restriction on both supply inverter and induction machine winding insulation considerations, the stator voltage is limited and maintained at a constant magnitude $U_s = U_N$ when $f_s > f_N$ and the induction machine operates in weakened flux conditions [1,5-11]. Since the stator flux and stator pulsation exhibit an inverse proportionality relation, the machine torque capability is strongly affected (see Figure 9). This is the reason for the limited increase of stator frequency.

Simultaneously, due to the decrease of flux ψ_s on the basis of the law "$1/\omega_s$":

$$\psi_s = \psi_{sN} \cdot \frac{\omega_N}{\omega_s} \approx \frac{U_N}{\omega_s} \tag{29}$$

a reduction of the maximum electromagnetic torque occurs, and its equation (4) at over-rated frequencies $f_s > f_N$ becomes:

$$M_{k\psi_s} = \frac{3p}{2} \cdot \frac{1-\sigma}{\sigma \cdot L_s} \cdot [\psi_{sN} \cdot \frac{\omega_N}{\omega_s}]^2 = M_{k\psi_{sN}} \cdot (\frac{\omega_N}{\omega_s})^2 \tag{30}$$

In this context, the maximum value of the stator frequency f_{smax} is established from the electromagnetic power invariance condition $P_M = M \cdot \Omega_s = M \cdot \omega_s/p$ (transferred by air-gap) at different over-rated values of stator frequency f_s.

In order to maintain a constant electromagnetic power $P_M = M \cdot \Omega_s = M \cdot \omega_s/p$ (at nominal level P_{MN} = ct.) even for the maximum stator frequency f_{smax}, the following relation can be written:

$$M_N \cdot \frac{\omega_N}{p} = M_{f_{smax}} \cdot \frac{\omega_{smax}}{p} \tag{31}$$

If at the maximum frequency f_{smax} the condition $M_{f_{smax}} = M_{k\psi_s}$ is imposed, the following results:

$$M_N \cdot \frac{\omega_N}{p} = M_{k\psi_{sN}} \cdot (\frac{\omega_N}{\omega_{smax}})^2 \cdot \frac{\omega_{smax}}{p} \quad \Rightarrow \quad \omega_{smax} = \frac{M_{k\psi_{sN}}}{M_N} \cdot \omega_N \tag{32}$$

or taking into account the definition of the torque overload capacity λ_M we obtain:

$$\lambda_M = \frac{M_{k\psi_{sN}}}{M_N} \quad \Rightarrow \quad f_{smax} = \lambda_M \cdot f_N \tag{33}$$

Consequently, the increase of the maximum frequency f_{smax} can be achieved through the design and further construction of induction machines with increased torque overload capacity λ_M. For traction induction machines, λ_M can take on values of 2.5 to 3.0.

3 Analysis of Electromagnetic Torque Developed by Traction Synchronous Motor

The electromagnetic torque M (respectively, the electromagnetic power $P_M = M \cdot \Omega$ with $\Omega = \omega/p$) developed by any synchronous motor is determined by calculation on basis of the active powers' balance, as follows [5,18]:

$$P_M = P_1 - p_{J1} = 3 \cdot U \cdot I \cdot \cos\varphi - 3 \cdot R_1 \cdot I^2 \tag{34}$$

$$M = \frac{P_M}{\Omega} = \frac{3 \cdot p}{\omega} \cdot (U \cdot I \cdot \cos\varphi - R_1 \cdot I^2) \tag{35}$$

Like a traction motor, the three-phase synchronous motor with salient poles is powered from a three-phase source, ideally with sinusoidal currents. In this case the current phasor $\underline{I}$ (through the reference stator winding) is specified by its magnitude $|\underline{I}|=I$ and the initial phase ψ to the axis q of the rotor, as in Figure 10. This means that implicitly the components I_d and I_q are specified of the stator current I [1,5,16,18].

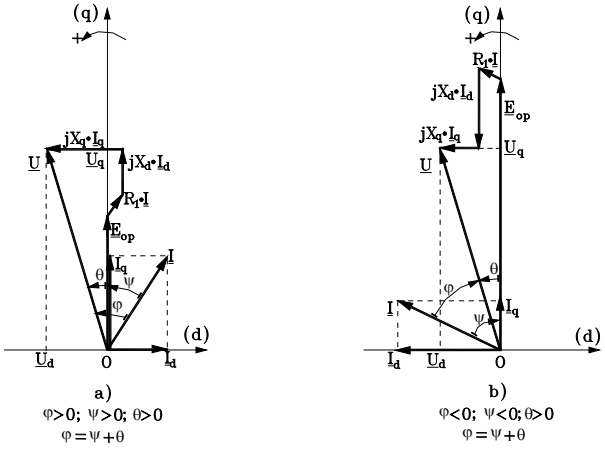

Figure 10. Blondel phasor diagram of synchronous motor with salient poles; a) under-excited operation (inductive current $\underline{I}$); b) over-excited operation (capacitive current $\underline{I}$)

In these conditions, the electromagnetic torque of the synchronous motor with salient poles M_I (at the current supplying) is determined as follows [1,5,16]:

$$M_I = \frac{3\cdot p}{\omega}[E_{0p}\cdot I\cdot\cos\Psi + (X_d - X_q)I^2\cdot\sin\Psi\cdot\cos\Psi] \quad (36)$$

which can be put in the final form [1]:

$$M_I = \frac{3\cdot p}{\omega}\cdot[E_{0p}\cdot I\cdot\cos\Psi + \frac{1}{2}I^2(X_d - X_q)\cdot\sin 2\Psi] \quad (37)$$

On the whole, the presence of two components $M_I = M_I' + M_I''$ is noticed.

The main component:

$$M_I' = \frac{3\cdot p}{\omega}E_{0p}\cdot I\cdot\cos\Psi$$

depends on the excitation degree (namely, the magnitude of excitation current I_e), while the secondary component:

$$M_I'' = \frac{3\cdot p}{\omega}\cdot\frac{I^2}{2}\cdot(X_d - X_q)\cdot\sin 2\Psi$$

is determined by the magnetic asymmetry of the rotor, being present (non-zero) even in the absence of the synchronous motor excitation. At I=ct., f=ct. and excitation current I_e=ct. (when E_{0p}=ct.), the electromagnetic torque M_I depends solely on the load angle ψ.

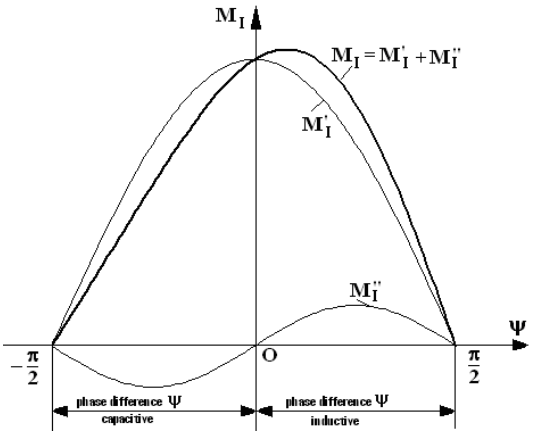

Figure 11. Characteristic representation $M_I = f(\psi)$ of synchronous motor with salient poles at powering from a three-phase source of sinusoidal currents

For the salient pole synchronous motor, the characteristic $M_I = f(\psi)$ is represented in Figure 11 by a thick line.

In the case of non-salient pole motors, in which $X_d=X_q=X_s$ the secondary component will not appear and the load characteristic $M_I = f(\psi)$ is represented just by the main component with a cosine variation.

Note that if in formula (37) of the torque M_I we make the following substitutions:

$$E_{0p} = \omega\cdot(w_1\cdot k_{w1}\frac{\Phi_{om}}{\sqrt{2}}); \quad X_d = \omega\cdot L_d \text{ and } X_q = \omega\cdot L_q \quad (38)$$

then the electromagnetic torque expression M_I (at the supply current) becomes:

$$M_I = 3p\cdot(w_1\cdot k_{w1}\frac{\Phi_{om}}{\sqrt{2}})\cdot I\cos\Psi + \frac{3p}{2}\cdot I^2(L_d - L_q)\cdot\sin 2\Psi \quad (39)$$

In relations (38) and (39) the physical significance of the new quantities follows:

w_1 = the number of turns, in series, on a stator phase of synchronous motor;

k_{w1} = the winding factor of a stator phase;

Φ_{om} = the maximum value of the main magnetic flux, depending on the magnitude of excitation current I_e, namely $\Phi_{om}=f(I_e)$;

L_d = the longitudinal inductance of stator winding;

L_q = the transverse inductance of stator winding of synchronous motor.

Particularly, for ψ=0 (when I_d=0 and I_q=I), the expression (39) of the electromagnetic torque M_I becomes:

$$M_I = M_I' = 3p(w_1\cdot k_{w1}\frac{\Phi_{om}}{\sqrt{2}})\cdot I = K\cdot\Phi_{om}\cdot I \quad (40)$$

so that M_I takes on a form that is mathematically identical to the electromagnetic torque $M=C_m\cdot\Phi\cdot I$ developed by a DC motor (with collector) with separated excitation. In relation (40), with K has been denoted the constructive constant $K = 3p\cdot w_1\cdot k_{w1}\frac{1}{\sqrt{2}}$ of the synchronous motor.

Expression (39) highlights that at I_e=ct., I=ct. and ψ=ct. the electromagnetic torque M_I is constant (and nonzero) and has the same magnitude regardless of the numerical value of the frequency f of the stator currents.

The existence of nonzero electromagnetic torque at the powering in current (by magnitude I phase shift ψ=ct. related to the counter-electromotive forces E_{op}) leads to the development of synchronous motor applications in electric traction.

On high speed electric trains, the traction synchronous motor is powered from a current inverter (thyristorised), with natural commutation, determined exactly by the counter-electromotive forces E_{op} (induced in the stator windings of the synchronous motor).

In this context one should recall that synchronous motor operation is characterized by a three-phase system of induced counter-electromotive forces ($-e_{0A}$, $-e_{0B}$, $-e_{0C}$) which might ensure the commutation of the three-phase bridge thyristors, just as the three-phase alternating voltage network ensured the commutation of rectifier bridge thyristors.

However, to ensure the natural commutation of the thyristorised bridge, the induced counter-electromotive forces must be of sufficiently large values, even at low speed, which requires the synchronous motor to run over-excited (from start up

to rated speed). The over-excitation of synchronous motor leads to winding currents I that are leading the voltage U (the phase shift φ being by capacitive type, like in Figure 3b), in this case the motor providing also through the terminals the reactive power necessary to the inverter bridge commutation.

In order to ensure the phase shift ψ (of the current fundamental I leading the counter-electromotive forces E_{op}), the control of the thyristors' conduction is based on the signals from a position transducer solidary with the rotor.

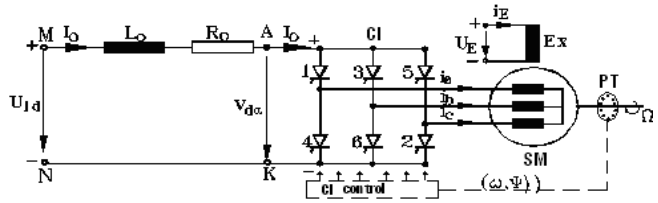

Figure 12. Self-piloted synchronous motor powered by a current inverter with natural commutation
SM = synchronous motor; Ex. = excitation winding; PT = position transducer
IC = three-phase current inverter; L_0, R_0 = inductance and resistance of smoothing coil

On the opposite side (the DC side) the autonomous current inverter (CI) must be connected to a DC variable source. Usually, a variable DC source is made up of adjustable DC voltage source (of chopper type or single-phase rectifier bridge with phase adjustment) connected in series with a smoothing coil with iron core, with the inductance L_0 of large size.

Accordingly, the configuration of a self-piloted synchronous motor powered from an autonomous current inverter is depicted in Figure 12 [5,16,18].

The representation entails the over-excited synchronous motor (SM), a three-phase thrystorised bridge (CI), a position transducer (PT) and a smoothing coil (with the parameters R_0 and L_0).

Since the supply is of current powered type, it is found that the reversibility of assembly SM+CI can only be achieved by changing the sign (by reversing the polarity) of the average voltage $V_{d\alpha}$ (on the DC side), thereby controlling the passing of three-phase bridge (CI) in rectifier regime.

3.1 Detection of Rotor Position

In contradistinction to the thyristorised bridge connected to three-phase network (thereupon the firing pulses of thyristors were synchronized with the alternating voltages of the network), for the current case of thyristorised bridge (through which the self-piloted synchronous motor is powered) the generation of firing pulses of thyristors must be correlated with the rotor position. Specifically, in the case of a synchronous motor with 2p magnetic poles, the rotor position controller must generate 6·p „control orders" (at each complete rotation of the rotor) for the ignition of thyristors of bridge CI. It should be noted that „the control orders" of the thyristor ignition are given evolutionary (with time) as the rotor rotates.

We note at this point that, in such circumstances, it is necessary to provide a device that will help operation of the thyristorised bridge, since that needs to piloting of knowing angular position of the rotor. To this purpose, the traction synchronous motor shall be provided with:

- a toothed steel disc, solidary with the rotor, precisely positioned relative to inductor poles, and
- a set of sensors, set on the stator and precisely positioned relative to the stator core slots.

The successive passing of teeth and slots of the toothed disc under the position sensors shall allow the determination at any time of the exact rotor position. Depending on the rotor position detected, the control is established of the thyristors supplying phase stator windings so that the electromagnetic torque developed by the motor is the maximum possible.

In principle, the stator sensors might be delayed in order to change the phase of control orders (of the ignition of thyristors) relative to the position of pole wheel. This way it is possible to control the phase angle ψ between the current and the induced counter-electromotive force on each phase. Nevertheless, on the modern traction synchronous motor the angle ψ is electronically controlled by an electronic phase shift of signals generated by the position sensors. Usually, the device to detecting the rotor position is located inside the traction synchronous motor, being situated on the opposite side to the rotor shaft end.

3.2 Diagram of currents for the traction synchronous motor

The synchronous motor will be over-excited and the three-phase induced counter-electromotive forces ($-e_{0A}$, $-e_{0B}$, $-e_{0C}$) of frequency $f=\omega/2\pi$ are able to drive the commutation of the current inverter thyristors at any speed $\Omega>\Omega_{min}$ without risk of losing synchronism between rotor and rotating magnetic field [1,4-6,9].

Specifically, at any speed "n" of the rotor of self-piloted synchronous motor (corresponding to the frequency $f=p\cdot n/60$ of stator currents) through the induced counter-electromotive forces the synchronous motor is piloting the converter which, from the DC current I_0, is distributing (on each of the three phases of the stator) current pulses of amplitude $\pm I_0$, duration T/3 and a repetition frequency $f=1/T=\omega/2\pi$ which is proportional to the angular mechanical speed of rotor rotation $\Omega=\omega/p$ (see Fig. 13).

The angular mechanical speed Ω of rotor results from the fundamental equation of motion:

$$J \cdot \frac{d\Omega}{dt} = M - M_{ex} \quad (41)$$

Under the simplifying assumption of a DC current I_0 that is perfectly smooth (when $L_0 \rightarrow \infty$) and neglecting the commutation durations, the stator currents i_a, i_b, şi, i_c (flowing through the phases of synchronous motor) will take on the forms of variation with time depicted in Figure 13.

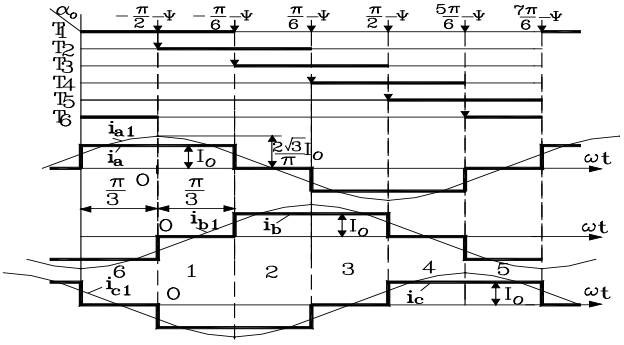

Figure 13. Conduction intervals of three-phase thyristor bridge and shapes of variation with time of currents i_a, i_b, şi, i_c (and their fundamentals i_{a1}, i_{b1}, şi, i_{c1})

In these conditions the fundamentals of stator currents (denoted by i_{a1}, i_{b1}, şi, i_{c1} in Figure 13) form a three-phase symmetrical current system (by direct sequence) with frequency $f=\omega/2\pi$ and the effective I_1 value given by:

$$I_1 = \frac{\sqrt{6}}{\pi} \cdot I_0 \quad (42)$$

3.3 Synchronization of commands

Operation of the self-piloted synchronous motor is based on ensuring the capacitive shift phase ψ=ct. between the space phasor of stator currents and the axis q. This condition is verified six times during each time period T (by controlling the moments of thyristor ignition relative to the position $\alpha=\omega t+\alpha_0$ of the axis d of the rotor). For this purpose, a position transducer TP provides the rotor positions (with respect to a reference direction of the stator) at which the bridge thyristors of the current inverter IC are on [5,8-10,16].

Ideally, for harmonic variation of stator currents, their space phasor $\underline{i}_{1dq}$ (in the rotor referential (d,q)) is a fixed phasor, mathematically expressed by:

$$\underline{i}_{1dq} = \sqrt{2} I_1 \cdot e^{j(\frac{\pi}{2}+\psi)} \quad (43)$$
$$with \quad I_1 = \frac{\sqrt{6}}{\pi} \cdot I_0$$

In the fixed stator referential the space phasor $\underline{i}_{1dq}$ matches the expression $\underline{i}_{1s}$:

$$\underline{i}_{1s} = \frac{2}{3}(i_{a1} + a\, i_{b1} + a^2 i_{c1}) = \underline{i}_{1dq} e^{j\alpha} = \frac{2\sqrt{3}}{\pi} I_0 \cdot e^{j(\frac{\pi}{2}+\psi+\alpha)} \quad (44)$$

with $\alpha = \omega t + \alpha_0$.

If the reference stator axis overlaps the magnetic axis of phase A, and the temporal origin (ωt=0) is chosen when the current i_{a1} (phase A) passes through a maximum (a moment that is coinciding with thyristor ignition timing), the space phasor $\underline{i}_{1s}$ will be of the form:

$$\underline{i}_{1s} = \sqrt{2} \cdot I_1 \cdot e^{j\omega t} = \sqrt{2} \cdot (\frac{\sqrt{6}}{\pi} I_0) \cdot e^{j\omega t} \quad (45)$$

From the expressions (38) and (39), it follows that:

$$\frac{\pi}{2} + \psi + \alpha_0 = 0 \Rightarrow \alpha_0 = -(\frac{\pi}{2} + \psi) \quad (46)$$

This angle represents the rotor position at the moment of ignition of thyristor T_2. The other thyristors will be switched on their natural succession (at successive positions of the rotor evenly shifted by π/3 electric radians) as in Figure 13.

3.4 Considering the sinusoidal currents

When considering only the fundamentals of stator current, the space phasor $\underline{i}_{1dq}$ (in the rotating referential d,q) is fixed and is subject to the expression (in polar form) given by (43). From this relationship, identifying the equivalent algebraic form:

$$\underline{i}_{1dq} = \sqrt{2} \cdot I_1 \cdot e^{j(\frac{\pi}{2}+\psi)} = \sqrt{2} \cdot (I_{1d} + j \cdot I_{1q}) \quad (47)$$

where the effective values I_{1d} and I_{1q} of the orthogonal components are:

$$I_{1d} = -I_1 \cdot \sin\psi = -(\frac{\sqrt{6}}{\pi} I_0)\sin\psi$$

$$I_{1q} = I_1 \cdot \cos\psi = (\frac{\sqrt{6}}{\pi} I_0)\cos\psi$$

If further in the expression of the electromagnetic torque M the following substitutions are performed: $I_d=I_{1d}$ and $I_q=I_{1q}$, the following result holds for $M=M_I$:

$$M_I = 3p[\frac{\sqrt{6}}{\pi} \cdot I_0 \cdot (K\Phi_{0m}) \cdot \cos\psi - \frac{3}{\pi^2} \cdot I_0^2 \cdot (L_d - L_q) \cdot \sin 2\psi] \quad (48)$$

where the average value of current I_0 (which is established in the DC intermediary circuit) is calculated from the relationship:

$$I_0 = \frac{U_{1d} - V_{d\alpha}}{R_0} \quad (49)$$

The sole problem of self-piloted synchronous motor is the starting regime [5,8-10,15-16]. At low rotational speeds, under 5% of Ω_{max}, the counter-electromotive force ($-e_{0p}$) becomes unable to ensure the commutation of the thyristors of the current inverter (CI). In this speed range, assisted commutation is

applied, usually realized by the device AC through creative options.

3.5 Considering the non-sinusoidal currents

In very deed, the phase currents i_a, i_b, i_c are strongly distorted as against the ideal sinusoidal shape [1,5,16]. Actually, under the simplifying assumptions adopted, each phase current (i_a, i_b or i_c from Fig. 13) consists of "rectangular blocks" of amplitude $\pm I_0$ (and duration equal to $2\pi/3$) separated by intervals (by duration $\pi/3$) in which the currents are null.

Moreover, the fundamentals of phase currents (denoted by i_{a1}, i_{b1} and i_{c1} in Figure 13) have equal amplitudes (of magnitude $\frac{2\sqrt{3}}{\pi} I_0$) and they are shifted, one lagging another, with the same angle of $2\pi/3$, forming a symmetrical three-phase system of sinusoidal currents, by direct succession. One could notice that by I_0 is denoted the DC intensity from the DC intermediary circuit.

In the fixed stator referential αβ, with the real axis Oα overlapped to reference stator winding axis A and with the temporal origin (ωt=0) chosen at the moment when its current is passing through a maximum (when $i_{a1} = \frac{2\sqrt{3}}{\pi} I_0$), the space phasor $\underline{i}_{1s}$ of stator current fundamentals, calculated with the formula:

$$\underline{i}_{1s}(\omega t) = \frac{2}{3} \cdot (i_{a1} + a \cdot i_{b1} + a^2 \cdot i_{c1}) = \sqrt{2}(\frac{\sqrt{6}}{\pi}) I_0 \cdot e^{j\omega t} \quad (50)$$

is a rotating phasor (with the angular speed ω=ct) with the top-point describing the circle of radius equal to $\sqrt{2}(\frac{\sqrt{6}}{\pi}) \cdot I_0 = \frac{2 \cdot \sqrt{3}}{\pi} \cdot I_0$ (represented by dashed line in Figure 13).

In the same time interval, still in the fixed stator referential αβ, the space phasor $\underline{i}_s$ (of non-sinusoidal currents) is completely different. For this reason, analytically it will proceed to an evaluation of this space phasor on each angular interval (by width $\pi/3$), in which the stator currents i_a, i_b and i_c remain constant. Thereby:

1. In the first interval $0 \le \omega t \le \pi/3$ when $i_a = +I_0$, $i_b = 0$ and $i_c = -I_0$ the space phasor $\underline{i}_s$ is fixed (position "0" in Figure 14) and has the expression:

$$\underline{i}_s(\omega t) = \frac{2}{3}(i_a + a \cdot i_b + a^2 \cdot i_c) = \frac{2}{3} \cdot (I_0 - a^2 \cdot I_0) = \frac{2}{\sqrt{3}} \cdot I_0 \cdot e^{j\frac{\pi}{6}}; \quad 0 \le \omega t < \frac{\pi}{3} \quad (51)$$

2. In the interval (k+1) by width $\pi/3$, when ωt may be written as:

$$\omega t = k \cdot \frac{\pi}{3} + \omega t'; \quad 0 \le \omega t' < \frac{\pi}{3}; \quad k = 1, 2, 3 \ldots \quad (52)$$

the space phasor $\underline{i}_s$ remains fixed (in position "k", k=1,2,3… in Figure 14) on whole duration $0 \le \omega t' < \pi/3$.

Broadly speaking, for any ωt by type (46), the expression of space phasor $\underline{i}_s$ can be written as:

$$\underline{i}_s(\omega t) = \frac{2}{\sqrt{3}} \cdot I_0 \cdot e^{j(\frac{\pi}{6} + k \cdot \frac{\pi}{3})} \quad (53)$$

with $k = 0, 1, 2, 3 \ldots$

During each period $\omega T = 2\pi$, the space phasor $\underline{i}_s(\omega t)$ of non-sinusoidal currents will successively scan all 6 fixed positions (denoted by "0", "1", "2", "3", "4", "5" in Figure 14). At each position it will remain motionless for

$$t' = \frac{\pi}{3\omega} = \frac{\pi}{3}\left[\frac{T}{2\pi}\right] = \frac{T}{6},$$

that time being numerically equal to the duration between two successive commutations of the bridge, then instantly "jumps" to the next position.

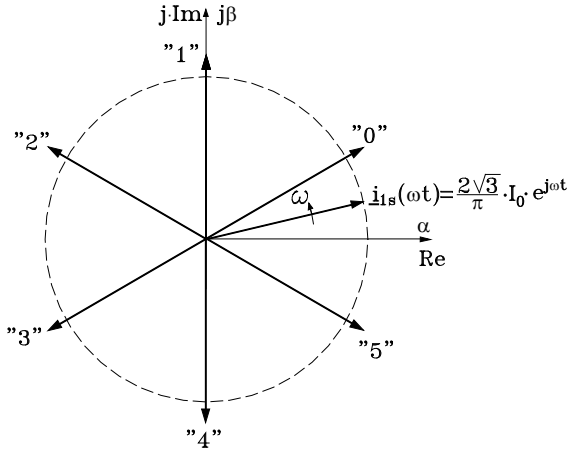

Figure 14. Rotating space phasor $\underline{i}_{1s}(\omega t)$ and the 6 fixed positions of non-sinusoidal current phasor $\underline{i}_s(\omega t)$ in the fixed stator referential

Geometrically, over the duration of each period $\omega T = 2\pi$, the "jumping" space phasor $\underline{i}_s(\omega t)$ performs a complete rotation, like the rotating phasor $\underline{i}_{1s}(\omega t)$ of current fundamentals [1,5]. Accordingly, the virtual angular speed ω_{vir} (fictitious average) of rotation of "jumping" phasor of non-sinusoidal currents $\omega_{vir} = \frac{2\pi}{T} = 2\pi f = \omega$ is numerically equal to the rotation angular speed ω of the rotating phasor of stator current fundamentals. Consequently, this common value ω of angular speeds will be used at changing the referential of space phasors.

In the coordinates (d,q) rotating with angular speed ω, the space phasor $\underline{i}_{1s}$ will become $\underline{i}_{1dq}$, while the space phasor $\underline{i}_s$ will become $\underline{i}_{dq}$. At changing the referential, the relations among these phasors are as the form:

$$\underline{i}_{1dq} = \underline{i}_{1s} \cdot e^{-j\alpha}; \quad \alpha = \alpha_0 + \omega t \quad (54)$$

$$\underline{i}_{dq} = \underline{i}_s \cdot e^{-j\alpha}; \quad \alpha = \alpha_0 + \omega t \tag{55}$$

With expression (50) for $\underline{i}_{1s}$, the relation of phasor $\underline{i}_{1dq}$ given by (54) takes on the form:

$$\underline{i}_{1dq} = \sqrt{2} \cdot (\frac{\sqrt{6}}{\pi}) \cdot I_0 \cdot e^{j\omega t} \cdot e^{-j(\alpha_0 + \omega t)} = \frac{2\sqrt{3}}{\pi} I_0 \cdot e^{-j\alpha_0} \tag{56}$$

Similarly, for any ωt of the form: $\omega t = k \cdot \frac{\pi}{3} + \omega t'$

with $0 \le \omega t' < \frac{\pi}{3}$.

and k = 0, 1, 2, 3, … when, in fixed coordinates, the space phasor $\underline{i}_s$ has the expression (53), it will result that, in synchronous rotating coordinates, the space phasor $\underline{i}_{dq}$ will be established by:

$$\underline{i}_{dq} = \frac{2}{\sqrt{3}} \cdot I_0 \cdot e^{j(\frac{\pi}{6} + k\frac{\pi}{3})} \cdot e^{-j(\alpha_0 + k\cdot\frac{\pi}{3} + \omega t')} = \frac{2}{\sqrt{3}} \cdot I_0 \cdot e^{j(\frac{\pi}{6} - \alpha_0 - \omega t')} \tag{57}$$

If the initial position α_0 it is chosen accordingly to relation (52), meaning $\alpha_0 = -(\frac{\pi}{2} + \psi)$, then in rotating coordinates (d,q), the space phasors $\underline{i}_{1dq}$ and $\underline{i}_{dq}$ become respectively:

$$\underline{i}_{1dq} = \frac{2\sqrt{3}}{\pi} \cdot I_0 \cdot e^{j(\frac{\pi}{2} + \psi)} = j \cdot \frac{2\sqrt{3}}{\pi} \cdot I_0 \cdot e^{j\psi} \tag{58}$$

$$\underline{i}_{dq} = \frac{2}{\sqrt{3}} \cdot I_0 \cdot e^{j(\frac{\pi}{2} + \psi + \frac{\pi}{6} - \omega t')} = j \cdot \frac{2}{\sqrt{3}} \cdot I_0 \cdot e^{j(\psi + \frac{\pi}{6} - \omega t')} \tag{59}$$

Space phasors $\underline{i}_{1dq}$ and $\underline{i}_{dq}$ are geometrically represented in Figure 15, in the interval $0 \le \omega t' < \frac{\pi}{3}$ (on the time duration $0 \le t < \frac{\pi}{3\omega} = \frac{\pi \cdot T}{3 \cdot 2\pi} = \frac{T}{6}$), meaning that exactly the duration T/6 between two successive commutations of the bridge.

Figure 15 emphasizes that during the time between two successive commutations T/6 the space phasor $\underline{i}_{dq}$ rotates in opposite sense, with the angular speed ω=ct., its extremity describing the arc between the points 1 and 2 corresponding to an angle at the centre of π/3 electrical radians [1,5,16].

At the moment t'=0, the phasor $\underline{i}_{dq}$ starts from initial position **1** (corresponding to angle $\psi+30^0$) towards the final position **2** (corresponding to angle $\psi-30^0$), reached after t'=T/6. At each commutation of the bridge, the space phasor $\underline{i}_{dq}$ instantly returns from position 2 to position 1, then the oscillation around the fixed phasor $\underline{i}_{1dq}$ is repeated in an identical manner.

Accordingly, the electromagnetic torque M_I developed by the self-piloted synchronous motor will oscillate.

In order to evaluate the electromagnetic torque M_I, we first establish the effective values $I_d(t')$ and $I_q(t')$ of the orthogonal components of phasor $\underline{i}_{dq}$:

$$\underline{i}_{dq} = \sqrt{2} \cdot [I_d(t') + j \cdot I_q(t')] = j \cdot \frac{2}{\sqrt{3}} \cdot I_0 \cdot e^{j(\psi + \frac{\pi}{6} - \omega t')} \tag{60}$$

Then, by identifying terms, the following immediately is observed:

$$I_d(t') = -\sqrt{\frac{2}{3}} I_0 \sin(\psi + \frac{\pi}{6} - \omega t') \tag{61}$$
$$I_q(t') = \sqrt{\frac{2}{3}} I_0 \cos(\psi + \frac{\pi}{6} - \omega t')$$

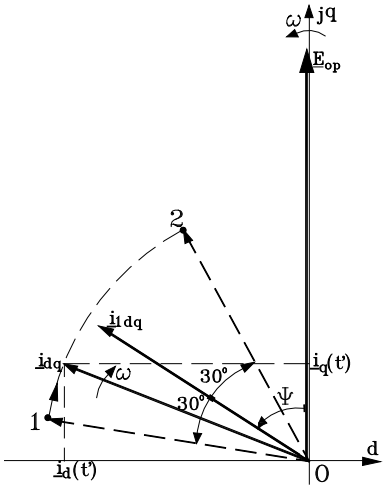

Figure 15. Oscillations of phasor $\underline{i}_{dq}$ around $\underline{i}_{1dq}$ in case of rectangular currents

If in expression (30) of the electromagnetic torque M there are performed the substitutions $I_d = I_d(t')$ and $I_q = I_q(t')$ specified by (51), then the torque M_I takes on the form:

$$M_I(t') = 3p \cdot \left[(K\Phi_{0m}) \cdot \sqrt{\frac{2}{3}} I_0 \cos(\psi + \frac{\pi}{6} - \omega t') - \frac{I_0^2}{3}(L_d - L_q) \sin 2(\psi + \frac{\pi}{6} - \omega t') \right] \tag{62}$$

This expression of the torque is valid in each interval $0 < \omega t' < \pi/3$ between two successive commutations of the bridge. Overall, the torque M_I is irregular.

The non-uniformity of electromagnetic torque M_I is caused by the variation of the orthogonal components $I_d(t')$ and $I_q(t')$, according to (37), this variation being determined by the oscillation of space phasor $\underline{i}_{dq}$ around the fixed phasor $\underline{i}_{1dq}$. On each period T (of non-sinusoidal variation of currents) the electromagnetic torque M_I performs six pulsations of the type described by relationship (62).

In order to attenuate pulsations of electromagnetic torque one is searching for ways to limit the oscillation amplitude of phasor $\underline{i}_{dq}$ (for instance between $\psi+15^o$ and $\psi-15^o$). For this goal, the stator winding of synchronous motor is divided in two distinct three-phase windings (spatially shifted with π/6 electrical radians), each being separately supplied from a current inverter. If the two inverters provide current pulses shifted from each other by π/6 electric

radians, then it could be achieved a system with the pulsation index q=2·6=12, consequently with a pulsation period of the electromagnetic torque equal to T/12. It follows implicitly that the amplitude of torque pulsation will be less.

4 Conclusion

Addressing the sustainability of operation of the AC traction electric motors constitutes a challenge in electric railway transportation research.

An electromagnetic torque capability analysis of the traction AC electric motors has been carried out in this study.

The analysis of the torque capability of the traction inductor motor emphasizes that the greatest magnitudes of electromagnetic torque are obtained for operation at a constant stator flux Ψ_s=ct. The study highlights that the maximum electromagnetic torque when the induction motor is operating at constant useful flux Ψ_u = ct. is approximately 20% smaller than the maximum torque when operating at Ψ_s = ct. Moreover, at the imposed electromagnetic torque, the smallest value of rotor pulsation is obtained for operation with Ψ_s = ct. The analysis of induction machine operation with constant flux highlights also that only at constant rotor flux Ψ'_r = ct. do the induction machine mechanical characteristics not have extremum points; rather they are straight lines. These linear characteristics are preferable for the applications which demand high sustainability dynamics in induction machine operation.

The study of traction synchronous motor emphasizes that electric traction drive systems using synchronous motors fed by current inverters provide high performance for high speed electric trains, in terms of both train dynamics and sustainability. With respect to the electromagnetic torque capability of the traction synchronous motor, the paper highlights that in order to synchronize the machine rotating field with the rotor (and avoiding the risk of losing the synchronism at any frequency value of stator currents) the synchronous motor will control the current inverter which is powering it, becoming in this way a self-piloted synchronous motor. Actually, the position of direct axis of synchronous motor rotor will be checked in an evolutionary sense in time (through position transducers) 6·p times during each complete rotation (at any value of rotor speed), by the ignition control of the thyristor of the current inverter bridge that is supplying the motor. Hence, the paper emphasizes that at electrically driven railway systems with traction synchronous motors the functions of amplitude adjustment are completely separate from those of the frequency control. As a consequence, the result is a simpler construction for both the power part and the control electronics of static converters.

The paper supports the findings that electric traction drive systems using three-phase induction and synchronous motors fed by variable voltage or current variable frequency inverters enhance the sustainable operation of electric railway trains. The results of this work may lead to enhancements of the main criteria for optimising the safe and efficient operation of railway electric traction systems.

References:

[1] Bulucea C.A., Nicola D.A., Rosen M.A., Mastorakis N.E., Bulucea C.A., Operation analysis of AC traction motors in terms of electromagnetic torque capability on sustainable railway vehicles, *MATEC Web of Conferences, Proc. 2016 Int. Conf. on Circuits, Systems, Communications and Computers (CSCC 2016)*, Corfu Island, Greece, 14-17 July, 2016, in press.

[2] Hernandez Rivas M., Messagie M., Hegazy O., Marengo L., Winter O., Van Mierlo L., Environmental impact of traction electric motors for electric vehicles applications. *The International Journal of Lyfe Cycle Assessment*, October 2015.

[3] Chen L., Wang J., Lombard P., Lazari P., Leconte V., High-efficiency electric motor for electric vehicle, *2012 Flux Conference - Cedrat*, Rome, Italy, October 17-18, 2012, Available at: http://www.cedrat.com/fileadmin/user_upload/cedrat_groupe/Publications/Publications/2012/10/08_High_Efficiency_Motor_Design_for_EV_PL_Uni_Sheffield.pdf , Accessed on August 10, 2016.

[4] Hashemnia N.M., Asaei B., Comparative study of using different electric motors in the electric vehicles, *Published in Electrical machines, IEEE Publisher, 2008, ICEM 2008, Proc. 18th International Conference on Electrical* machines, Vilamoura, 6-9 Sept.2008, pp.1-5, Available at: https://www.researchgate.net/publication/224394177_Comparative_study_of_using_different_electric_motors_in_the_electric_vehicles , Accessed on August 12, 2016.

[5] Nicola D.A., *Tractiune electrica (Electric Traction)*, Universitaria Publishing House, Craiova, Romania (2012).

[6] Rosen M.A., Nicola D.A., Bulucea C.A., Cismaru D.C, Sustainability Aspects of Energy Conversion in Modern High-Speed Trains with

Traction Induction Motors, *Sustainability* **2015**, *7(3):* 3441-3459.

[7] Bulucea C.A., Nicola D.A., Mastorakis N.E., Rosen M.A., Understanding Electric Industrial Ecosystems through Exergy", *Recent Researches in Energy & Environment, Proc. of 6th IASME/WSEAS International Conference on Energy & Environment*, University of Cambridge, Cambridge, UK, February 23-25, 2011, pp. 182-191.

[8] Kaller R., Allenbach J.M., *Traction Electrique (Electrical Traction)*, Vol. 1-2, PPUR, Lausanne (1995).

[9] Perticaroli F, *Sistemi elettrici per i transporti: Trazione elettrica (Electrical Systems for Transportation: Electric Traction)*. Ed. Masson, Milano-Parigi-Barcellona (1994).

[10] Lozano J.A., Félez J., de Dios Sanz J., Mera J.M., *Railway Traction, Reliability and Safety in Railway*, Dr. Xavier Perpinya (Ed.), (2012), Available at: http://www.intechopen.com/books/reliability-and-safety-in-railway/railway-traction , Accessed on 15 February 2016.

[11] Bulucea C.A., Nicola D.A., Rosen M.A., Mastorakis N.E., Bulucea C.A., Modelling Examples of Sustainable Electric Power Equipment, *Recent Advances in Environmental and Earth Sciences and Economics, Proc. 2015 Int. Conf. on Energy, Environment, Development and Economics (EEDE 2015)*, Zakynthos Island, Greece, 16-20 July, 2015, pp. 108-115.

[12] Rosen M.A., A Concise Review of Energy-Based Economic Methods, *Proc. 3rd IASME/WSEAS Int. Conf. on Energy & Environment*, Cambridge, UK, Feb. 23-25, 2008, 136-142.

[13] Dincer I., Rosen M.A., *Exergy: Energy, Environment and Sustainable Development*, 2d ed., Elsevier: Oxford, UK (2013).

[14] Nicola D.A., Rosen M.A., Bulucea C.A., Brandusa C., Sustainable Energy Conversion in Electrically Driven Transportation Systems, *Proc. 6th WSEAS Int. Conf. on Engineering Education (EE'09)*, Rhodes, Greece, July 22-24, 2009, pp. 124-132.

[15] Georgescu M, *Tracţiunea electrică de mare viteză cu motoare sincrone (High Speed Electric Traction with Synchronous Motors)*, Dacia Publishing House, Cluj-Napoca (2001).

[16] Bulucea C.A., Nicola D.A., Cismaru D.C., Mastorakis N.E., Bulucea C.A., Brindusa C., Embedding sustainability dynamics in energy conversion chain on electric railway vehicles with traction synchronous motors, *Advances in Environmental Sciences, Development and Chemistry, Proc. 2014 Int. Conf. on Energy, Environment, Development and Economics (EEDS 2014)*, Santorini Island, Greece, July 17-21, 2014, pp. 21-28.

[17] Chatelain J., *Machines électriques (Electrical Machines)*, PPUR, Lausanne (1989).

[18] Nicola D.A., Bulucea C.A., *Electrotechnics, Electrical Equipment and Machines*, Vol. II "Electrical Equipment", SITECH Publishing House, Craiova (2005).